Cancer Immunology, Immunotherapy (2023) 72:1523–1539
https://doi.org/10.1007/s00262-022-03348-5

RESEARCH

Porphyromonas gingivalis promotes the progression of oral squamous cell carcinoma by activating the neutrophil chemotaxis in the tumour microenvironment

Zhi-chen Guo[1] · Si-li Jing[2] · Sakendeke Jumatai[1] · Zhong-cheng Gong[1]

Received: 6 September 2022 / Accepted: 5 December 2022 / Published online: 14 December 2022

Abstract

Background We aimed to determine the significance of *Porphyromonas gingivalis (P. gingivalis)* in promoting tumour progression in the tumour microenvironment (TME) of oral squamous cell carcinoma (OSCC).

Methods The Gene Expression Omnibus (GEO) was used to screen out the differentially expressed genes from the two datasets of GEO138206 and GSE87539. Immunohistochemistry and immunofluorescence analysis of samples, cell biological behaviour experiments, and tumour-bearing animal experiments were used to verify the results in vivo and in vitro. The mechanism was revealed at the molecular level, and rescue experiments were carried out by using inhibitors and lentiviruses.

Results CXCL2 was selected by bioinformatics analysis and was found to be related to a poor prognosis in OSCC patients. Samples with *P. gingivalis* infection in the TME of OSCC had the strongest cell invasion and proliferation and the largest tumour volume in tumour-bearing animal experiments and exhibited JAK1/STAT3 signalling pathway activation and epithelial-mesenchymal transition (EMT). The expression of *P. gingivalis*, CXCL2 and TANs were independent risk factors for poor prognosis in OSCC patients. A CXCL2/CXCR2 signalling axis inhibitor significantly decreased the invasion and proliferation ability of cells and the tumour volume in mice. When lentivirus was used to block the CXCL2/CXCR2 signalling axis, the activity of the JAK1/STAT3 signalling pathway was decreased, and the phenotype of EMT was reversed.

Conclusion *Porphyromonas gingivalis* promotes OSCC progression by recruiting TANs via activation of the CXCL2/CXCR2 axis in the TME of OSCC.

Keywords *Porphyromonas gingivalis* · Oral squamous cell carcinoma · Chemokine · EMT · Prognosis · Periodontal disease

Abbreviations

GEO	Gene Expression Omnibus
OSCC	Oral squamous cell carcinoma
TANs	Tumour—associated neutrophils
P. gingivalis	*Porphyromonas gingivalis*

Introduction

Oral squamous cell carcinoma (OSCC) is the most common malignancy of the head and neck, accounting for more than 800,000 new cases and 450,000 deaths in 2018 worldwide [1]. In the USA, 54,010 new OSCC cases were diagnosed, and 10,850 patients died from OSCC in 2021 [2]. OSCC has gradually become a serious problem worldwide, and despite the rapid development of clinical treatment in the past few decades, the 5-year survival rate of this disease has not significantly improved [3]. An increasing number of microorganisms have been reported to be strongly associated with human carcinogenesis, such as *Helicobacter pylori* in gastric cancer [4]. Nevertheless, how oral microorganisms influence the tumour microenvironment (TME) and how they promote tumour development remain unknown.

Porphyromonas gingivalis (*P. gingivalis*) is a key pathogen in periodontal disease, which has been regarded as an independent microorganism for tumour progression and

✉ Zhong-cheng Gong
gump0904@aliyun.com

[1] Oncological Department of Oral and Maxillofacial Surgery, The Affiliated Stomatology Hospital of The First Affiliated Hospital of Xinjiang Medical University, Xinjiang Uygur Autonomous Region Institute of Stomatology, No.137, Li Yu Shan South Road, Urumqi 830054, Xinjiang, People's Republic of China

[2] Department of Ophthalmology, The First Affiliated Hospital of Xinjiang Medical University, Urumqi, China

may increase the risk of mortality in patients with OSCC [5]. In addition, gastrointestinal cancers have been found to be associated with *P. gingivalis*; for example, *P. gingivalis* infection could induce aggressive progression of oesophageal squamous cell carcinoma (ESCC) and gastric cancer [6]. The oral microbiome is closely related to the development of periodontal disease, although limited research has shown that the oral microbiome could also play an essential role in OSCC through direct metabolism of chemical carcinogens and general inflammatory effects [7]. The relationship between OSCC and inflammation has been seriously examined recently. During the inflammatory response, chemokines mediate leukocyte chemotaxis to OSCC sites to activate the local immune response against cancer lesions. However, prolonged inflammation contributes to the development of cancer [8].

Polymorphonuclear neutrophils (PMNs) are the primary defence line of the immune system and account for 70% of circulating leukocytes[9]. Tumour-associated neutrophils (TANs) infiltrate the TME, and there are two polarization types of TANs: N1 (tumour suppressive) and N2 (tumour promoting); the phenotype of TANs depends on the stage of tumour progression [10]. TANs are primarily activated by CXC chemokines [11], and *P. gingivalis* induces immune cells to secrete chemokines to promote tumour growth [12].

Chemokines play a role in chemical signalling during cell activation and differentiation, as well as in the process of movement, and their signalling receptors are important in the TME of OSCC [13]. CXCL2 is a type of small molecular proinflammatory chemokine that plays a role in coding protein secretion, immune regulation and the promotion of tumours [14]. CXCL2/CXCR2 is known to promote the chemotaxis of PMNs and contribute to the transformation and progression of tumours [15]. The Janus kinase signal transducer and activator of transcription (JAK/STAT) signalling pathway regulates almost all immune processes, and STAT3-driven tumorigenesis is primarily due to the loss of immune signals and the induction of inflammatory responses [16]. In the TME, the JAK1/STAT3 signalling pathway induces the transendothelial migration of tumour cells and macrophages into the TME, and the condition of the TME is changed by the secretion of chemokines [17]. In the TME of OSCC, whether the activity of the JAK1/STAT3 pathway can be activated by periodontal microbes and how to regulate this pathway remain unknown.

In this research, we identified the tumour-promoting role of *P. gingivalis* in OSCC. We also illustrated that *P. gingivalis* could promote TANs chemotaxis and further target CXCL2/CXCR2 in the TME of OSCC to accelerate the proliferation and invasion of OSCC cells, which worsens the patient's prognosis. These results indicate that TANs chemotaxis by *P. gingivalis* and targeting CXCL2/CXCR2 might be useful in combating OSCC progression. A high level of *P. gingivalis* could be a useful clinical indicator that doctors can use to assess OSCC patient prognosis.

Table 1 Primer sequence of qRT-PCR

Name of bacterial and genes	Primer sequence (3′→5′)	Reference
P. gingivalis	F: TGTAGATGACTGATGGTG AACC	Lee et al. [38]
	R: ACGTCATCCACACCTTCCTC	
CXCL2	F: ATCCAAAGTGTGAAGGTG AAGTC	
	R: CCCATTCTTGAGTGTGGC TATG	
CXCR2	F: GCCATGGACTCCTCAAGATT	
	R: AAGTGTGCCCTGAAGAAGAG	
GAPDH	F: GGGAAACTGTGGCGTGAT	
	R: AAAGGTGGAGGAGTGGGT	

P. gingivalis, Porphyromonas gingivalis; CXCL2, C-X-C motif chemokine ligand 2; CXCR2, C-X-C motif chemokine receptor 2

Materials and methods

Clinical samples

One hundred and forty formalin-fixed, paraffin-embedded blocks of OSCC samples and twenty normal samples were collected from the Oncology Department of Oral and Maxillofacial Surgery of The First Affiliated Hospital of Xinjiang Medical University (Urumqi, China) between March 2010 and March 2021. The patients general information including gender, age, living status, differentiation, T stage, N stage, clinical stage and recurrence, and the primary tumour located in the lips, palate, buccal, floor of mouth, tongue and gingiva. The patient sample was comprised of 88 males and 52 females, with a mean age of 63 years (ranging from 27 to 83 years). The use of OSCC samples was approved by the ethics review board (approval no. IACUC20180411-13). The TNM and clinicopathological classification and staging of patients with OSCC were performed according to the American Joint Committee on Cancer (No. 8 version of AJCC) guidelines.

Bioinformatics analyses

The GSE87539 [18] and GSE138206 [19] data were downloaded from Gene Expression Omnibus (GEO; http://www.ncbi.nlm.nih.gov/geo). The probe ID was converted into an international standard name for gene symbols using perl programming, and the gene expression matrix of the two datasets was merged by perl language also. The data normalized

were used by R language "sva" and "limma" packages, the differentially expressed genes (DEG) were filtered by "limma" package and using a cutoff criterium of adj. *P*. Val < 0.05 and |log2 (fold change)| > 2. The Gene Ontology (GO) and Kyoto Encyclopedia of Genes and Genomes (KEGG) enrichment analysis were used by R language "colourspace" and "string" packages, and Bioconductor packages ("DOSE", "clusterProfiler" and "pathview"). The PPI network of DEGs using online database STRING version 11 (https://string-db.org/) and the combining score > 0.9 were used for the PPI network construction. The top 30 hub genes were visualized by using Cytoscape software. Gene set enrichment analysis (GSEA) was used to evaluate the gene function between treated and control groups.

Immunohistochemistry (IHC) and immunofluorescence (IF) evaluation

OSCC samples and normal oral mucosa samples were harvested from humans and mice for HE staining and IHC; the methods for HE and IHC were described in our previous study [20]. Samples for IHC and IF were embedded in the paraffin and sectioned into 4-μm sections. IHC and IF were performed with anti-*P. gingivalis* (Dia-An, lnc, 1:200), anti-CXCL2 (bs-1162R, BIOSS, 1:500) and anti-TANs ($CD66b^+$, ab197678, Abcam, 1:500) antibodies. The immune expression of TANs in mice was assessed with an antibody against $CD11b^+$ (bs-1014R, BIOSS, Biotech, Beijing, China, 1:500) [21]. Image-Pro Plus version 6.0 software (Media Cybernetics, Inc., Bethesda, MD, USA) was used to evaluate the IHC expression levels. The IOD/total area of each field was also calculated simultaneously. According to the IOD value, the staining proportions (PS) were divided into: 0 (–), 1 (+), 2 (++), and 3 (+++). Four levels: 0 (0%); 1 (1–25%); 2 (26–50%); 3 (51–75%); and 4 (76–100%) were divided by the staining proportion score (PS). The intensity score (IS) multiplied by PS was the final result of the staining score [22]. The expression level was categorized into a low expression group (0–6) and a high expression group (7–12) in this study.

Bacterial and cell culturing

The *P. gingivalis* ATCC33277 strain was purchased from The American Type Tissue Culture Collection (ATCC), and the bacteria were grown in two culture systems: (1) Columbia liquid medium (purchased from Bei-Na Biotech, Inc., Beijing, China) and (2) Columbia blood agar culture medium (purchased from Bei-Na Biotech, Inc., Beijing, China). The human OSCC cell line TSCCa was provided by the Central Laboratory of First Affiliated Hospital of Xinjiang Medical University. TSCCa cells were maintained in RPMI 1640 (Thermo Fisher Scientific, CA, USA) containing 10% FBS (Thermo Fisher Scientific, CA, USA), penicillin and streptomycin (100 μg/ml) (Thermo Fisher Scientific, CA, USA). The coculture cell model (*P. gingivalis* and TSCCa) was established with a multiplicity of infection (MOI) of 50 and when the coculture model was established, the penicillin and streptomycin were removed from the medium. Human TANs were extracted from the peripheral blood of OSCC patients with a human peripheral blood neutrophil isolation kit (Solarbio, Biotech, Inc., Beijing, China). We used MOI of 50 and incubation for 48 h is because that we have established the coculture model according to the different MOI, (for example: 1, 10, 50 and 100) and in the different time points (for example: 12, 24, 36 and 48 h) through the pre-experiment, we found that when TSCCa cells were under the MOI of 50, not only *P. gingivalis* could affect it, but also in the best state (Fig. S1). TANs were added to the coculture cell model at 1:1 ratio (TSCCa: TANs), we selected 1:1 ratio was used for subsequent studies is because that in the pre-experiment process, we have set the different ratios (for example: 1:1, 1:5, 1:10 and 1:50) and finally we found that the invasion, migration and proliferation ability of TSCCa in the cell models is the strongest under the 1:1 ratio (Fig. S2).

Fluorescent staining of cell coculture model

Bacterial staining: *P. gingivalis* was marked by the fluorochrome of SYTO9 Green Fluorescent Nucleic Acid Stain (Thermo Fisher Scientific, CA, USA). Nuclear staining was performed with DAPI (Bioss, Biotech, Inc., Beijing, China). Cellular mitochondrial staining was marked by MitoTracker red (Beyotime Biotech, Inc., Beijing, China). The coculture cell model was established at an MOI of 50 in a 37 °C incubator for 48 h, and confocal laser photography was performed.

Neutrophil chemotaxis assay

We used Transwell chambers (Corning, Bioscience, NY, USA) with 5-μm polycarbonate membranes. Briefly, TANs were treated with the supernatant of different groups, and the supernatant was placed into the bottom chamber. TANs suspended in RPMI 1640 containing 2% FBS (1×10^5 cells/100 μL) were added to the upper wells and incubated for 2 h in a 37 °C incubator. We collected TANs that migrated to the lower chamber and counted them after staining with crystal violet.

Cell Counting Kit-8 (CCK-8) assay

Cell proliferation was evaluated by CCK-8 assay (Keygen Biotech, China) following the manufacturer's instructions.

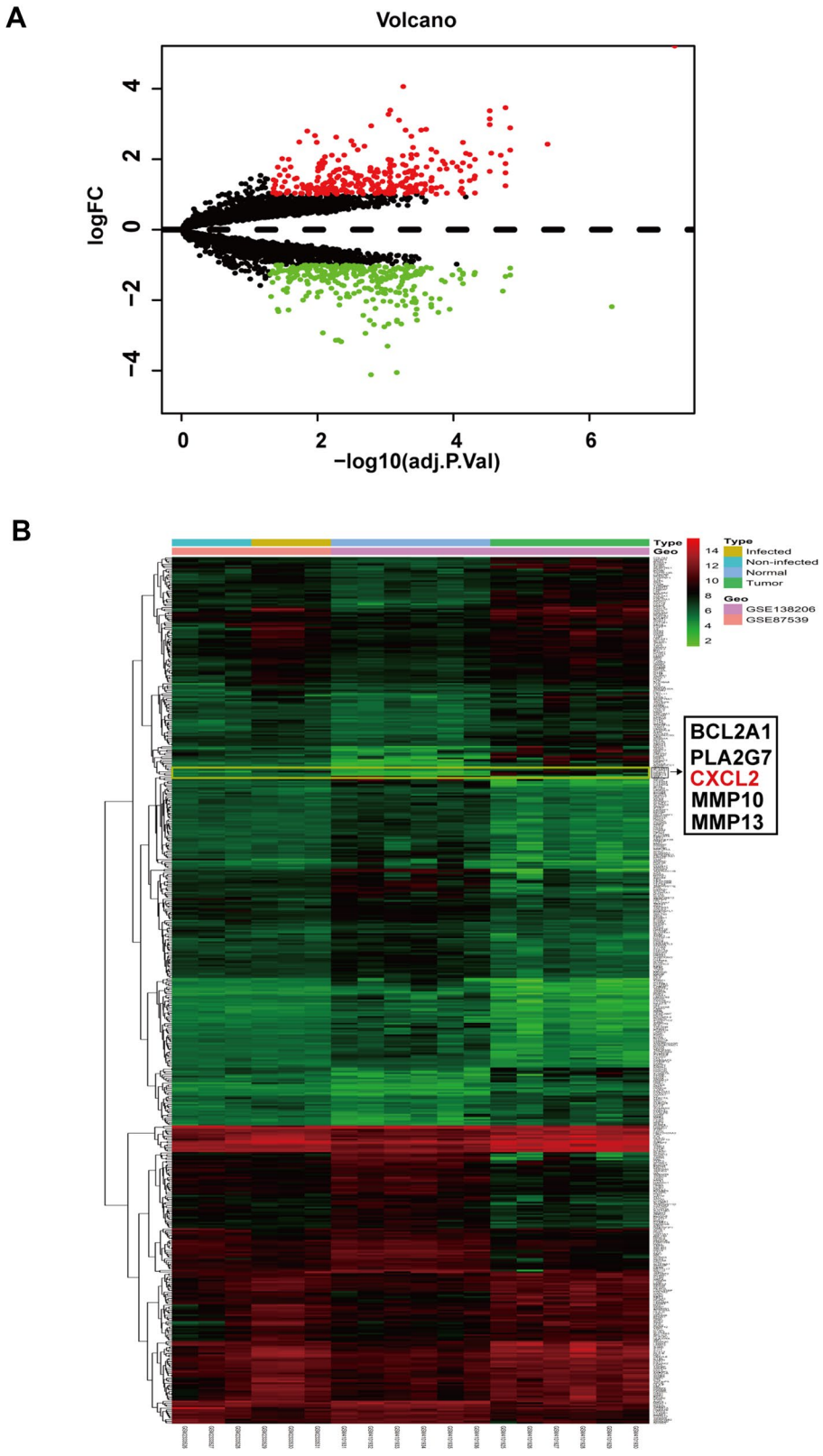

Fig. 1 DEGs identified in GSE138206 and GSE87539. Volcano map of DEGs between *P. gingivalis*-infected OSCC samples and uninfected normal oral mucosa samples. **a** The red points in the volcano plots represent upregulation and the green plots represent downregulation. **b** Heatmap of the total DEGs according to the value of |logFC|. The colour in heat map from green to red shows the progression from low expression to high expression

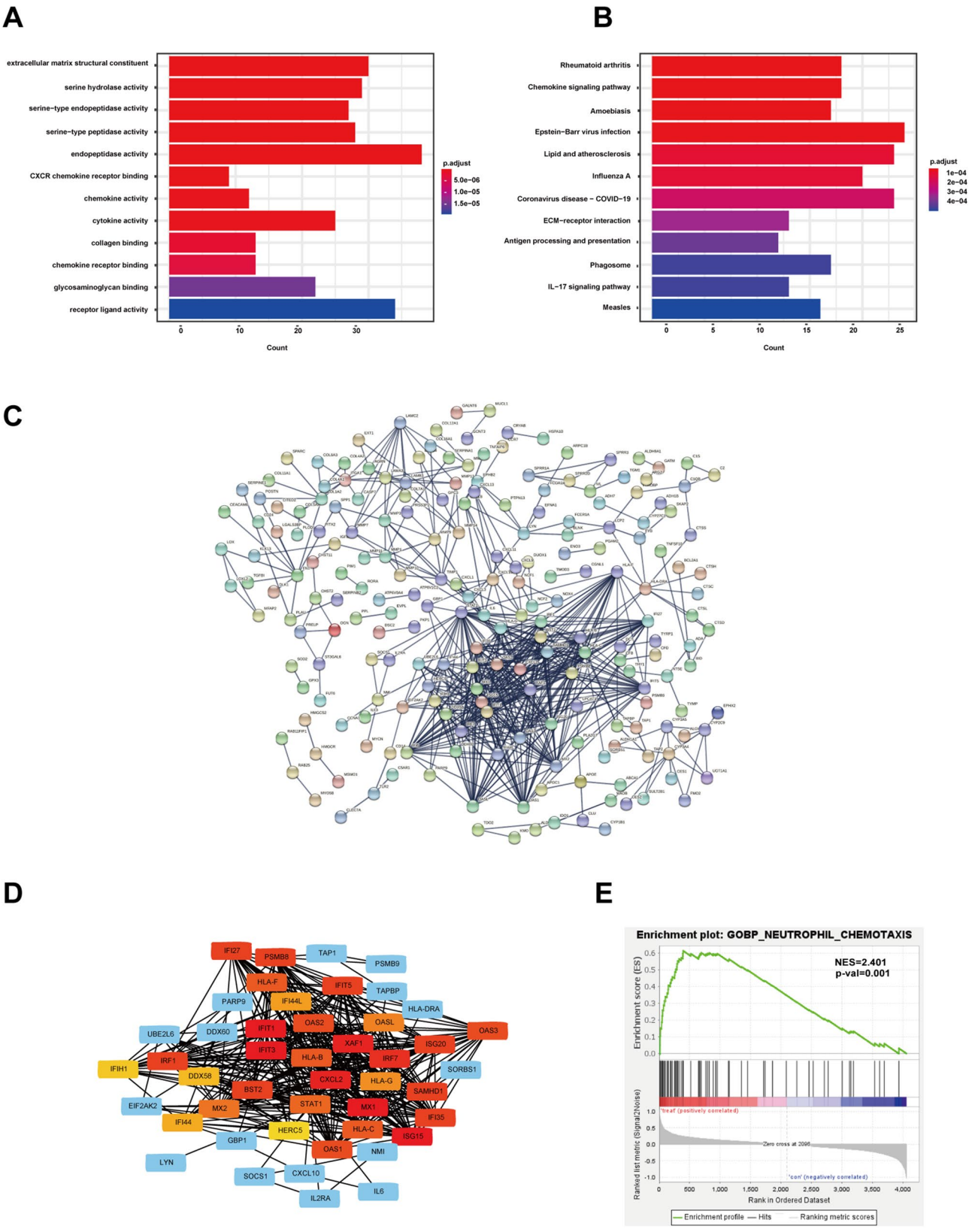

Fig. 2 Gene function enrichment analysis were conducted through the KEGG, GO and GSEA. **a** CXCR chemokine receptor binding, chemokine activity and chemokine receptor binding were enriched by GO analysis. **b** Chemokine signalling pathway was enriched by KEGG analysis. **c**, **d** CXCL2 was a key hub gene and located in the centre of the molecular interaction network by PPI and Cytoscapy. **e** Neutrophil chemotaxis was enriched by GSEA analysis

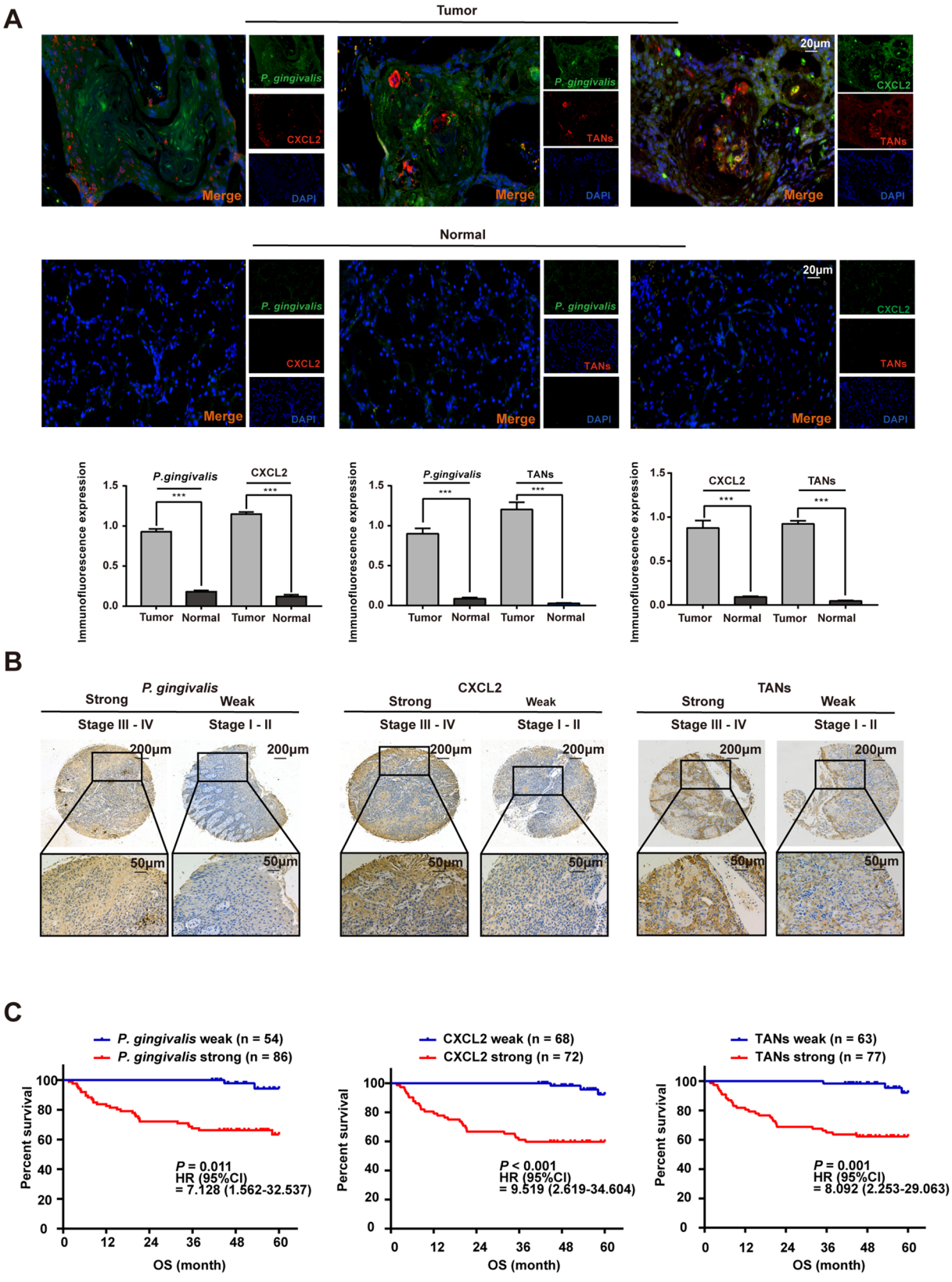
A
Tumor
P. gingivalis
CXCL2
DAPI
Merge
TANs
20μm
Normal
Immunofluorescence expression
P.gingivalis
CXCL2
TANs
***
Tumor
Normal
B
P. gingivalis
Strong
Weak
Stage III - IV
Stage I - II
200μm
50μm
CXCL2
TANs
C
P. gingivalis weak (n = 54)
P. gingivalis strong (n = 86)
Percent survival
P = 0.011
HR (95%CI)
= 7.128 (1.562-32.537)
OS (month)
CXCL2 weak (n = 68)
CXCL2 strong (n = 72)
P < 0.001
HR (95%CI)
= 9.519 (2.619-34.604)
TANs weak (n = 63)
TANs strong (n = 77)
P = 0.001
HR (95%CI)
= 8.092 (2.253-29.063)

◂**Fig. 3** The levels of *P. gingivalis*, CXCL2 and TANs were analysed by IHC and IF in the OSCC and normal samples, and IHC expression levels are correlated with the prognosis of OSCC patients. **a** The levels of *P. gingivalis*, CXCL2 and TANs and their relationships in OSCC and normal samples were detected by double-label IF. **b** The levels of *P. gingivalis*, CXCL2 and TANs in OSCC samples samples were detected by IHC. **c** Correlation analysis of the expression levels of *P. gingivalis*, CXCL2 and TANs between OSCC patients deaths (**$p < 0.01$, and ***$p < 0.001$; Student's *t*-test)

Ten microlitres of CCK-8 were added to each well. The 96-well plates were incubated for 2 h at 37 °C, and wells with only RPMI 1640 medium were used as blank controls. The absorbance of the coloured solution was quantified at 450 nm using a microplate reader (Tecan, Untersbergstrasse, Austria).

Invasion assay

Basement Matrigel membrane (BD Biosciences, CA, USA) was used to precoat the Transwell chamber with a filter with 8-μm pores (Corning, Bioscience, NY, USA); 2×10^5 cells from 5 different groups were suspended in FBS-free medium and seeded on the upper chamber. In the lower chamber, medium containing 10% FBS was added. Forty-eight hours later, the medium was aspirated, and the cells on the upper chamber were wiped away. The cells on the lower surface of the filter were counted after staining with crystal violet.

Enzyme-linked immunosorbent assay (ELISA)

To detect the level of CXCL2 in cell culture supernatants, we used the corresponding Quantikine Human ELISA Kit (Boster Biotech, Inc., Wuhan, China) in accordance with the manufacturer's instructions. The absorption was measured at 450 nm on a Thermo Scientific microplate reader. The assay can determine the levels in unknown samples according to the standard curve, which is made based on the absorption values of the standard sample.

OSCC mouse model

C57BL/6 mouse OSCC models were created with SCC7 cell lines, and all animal protocols were approved by the Animal Care Committee. The mice were divided into 4 groups, the treatment groups were injected with different doses of SCH527123 (SCH527123 is a novel and selective CXC chemokine receptor 2 [CXCR2] antagonist, which binds CXCR2 on neutrophils, inhibits neutrophil activation, modulates the neutrophil recruitment by CXC chemokine, [No. HY-10198, MCE, Inc., NJ, USA]) [39] in the tumour cell site at 4, 8, 12 and 16 days. The mice were killed at 20 days. The tumour tissue was removed for volume calculation, IHC and IF studies.

Transfection of lentiviral vectors

Recombinant lentiviruses named sh-CXCL2 and sh-CXCR2 were used to interfere with CXCL2/CXCR2 axis expression, and two empty carrier lentiviruses were used as negative controls. The lentivirus was purchased from GeneChem Biotech, Inc. (Shanghai, China). The cells were incubated with lentivirus for 48 h and screened with puromycin.

RNA isolation and quantitative real-time PCR

Total RNA was isolated from cells according to the TRIzol method (Invitrogen, Carlsbad, CA) in accordance with the manufacturer's instructions. We measured mRNA expression in cells via qRT-PCR. qRT-PCR was performed using the SYBR Prime Script RT-PCR Kit (Thermo Fisher Scientific, CA, USA) in accordance with the manufacturer's instructions. We used GAPDH as an internal control. The primers used are listed in Table 1.

Western blot analysis

The same amounts of protein samples (40 μg each) were separated by 12% sodium dodecyl sulphate polyacrylamide gel electrophoresis for 150 min at 75 V, and then the proteins were transferred to polyvinylidene difluoride (PVDF) membranes for 2 h at 100 V; the membranes were incubated in blocking buffer (5% milk in 1 × tris-buffered saline [TBS]) for 1 h at room temperature. The PVDF membranes were rocked in 1:1,000 primary antibody solution for at least one overnight at 4 °C. Then, the PVDF membranes were incubated in 1:1,000 secondary antibody solution for 1 h at room temperature. The results were visualized with chemiluminescent HRP substrate (Millipore, MA). Primary antibodies against *P. gingivalis* (Dia-An, lnc, it was freshly prepared, 1:1000), CXCL2 (bs-1162R, BIOSS, Biotech, Beijing, China, 1:2000), CXCR2 (bs-1629R, BIOSS, Biotech, Beijing, China, 1:2000), JAK1 (bs-1439R, BIOSS, Biotech, Beijing, China, 1:2000), STAT3 (bs-55208R, BIOSS, Biotech, Beijing, China, 1:2000), p-JAK1 (bs-3238R, BIOSS, Biotech, Beijing, China, 1:2000), p-STAT3 (bs-1658R, BIOSS, Biotech, Beijing, China, 1:2000), E-cadherin (bs-10009R, BIOSS, Biotech, Beijing, China, 1:2000), N-cadherin (bs-1172R, BIOSS, Biotech, Beijing, China, 1:2000), and GAPDH (bs-13282R, BIOSS, Biotech, Beijing, China, 1:2000) and secondary antibodies (anti-rabbit-HRP, Cell

Table 2 Immunohistochemical expression of *P. gingivalis*, CXCL2 and TANs in samples from 140 patients with oral squamous cell carcinoma according to clinical data and follow-up

Variable	*P. gingivalis*		*p*	CXCL2		*p*	TANs		*p*
	Weak	Strong		Weak	Strong		Weak	Strong	
Gender			0.460			0.795			0.888
Male	36 (40.9)	52 (59.1)		42 (47.7)	46 (52.3)		40 (45.5)	48 (54.5)	
Female	18 (34.6)	34 (65.4)		26 (50.0)	26 (50.0)		23 (44.2)	29 (55.8)	
Age			0.784			0.902			0.800
< 60 years	17 (37.0)	29 (63.0)		22 (47.8)	24 (52.2)		20 (43.5)	26 (56.5)	
≥ 60 years	37 (39.4)	57 (60.6)		46 (48.9)	48 (51.1)		43 (45.7)	51 (54.3)	
Living Status			< 0.001			< 0.001			< 0.001
Living	52 (48.1)	56 (51.9)		65 (60.2)	43 (39.8)		60 (55.6)	48 (44.4)	
Dead	2 (6.3)	30 (93.8)		3 (9.4)	29 (90.6)		3 (9.4)	29 (90.6)	
Differentiation			0.495			0.090			0.436
Poor-moderately	18 (42.9)	24 (57.1)		25 (59.5)	17 (40.5)		21 (50.0)	21 (50.0)	
Well	36 (36.7)	62 (63.3)		43 (43.9)	55 (56.1)		42 (42.9)	56 (57.1)	
T Stage			< 0.001			< 0.001			< 0.001
T1–2	49 (55.1)	40 (44.9)		62 (69.7)	27 (30.3)		58 (65.2)	31 (34.8)	
T3–4	5 (9.8)	46 (90.2)		6 (11.8)	45 (88.2)		5 (9.8)	46 (90.2)	
N Stage			< 0.001			< 0.001			< 0.001
N0	34 (68.0)	16 (32.0)		32 (64)	18 (36.0)		32 (64)	18 (36.0)	
N+	34 (37.8)	56 (62.2)		31 (34.4)	59 (65.6)		31 (34.4)	59 (65.6)	
Clinical Stage			< 0.001			< 0.001			< 0.001
I–II	29 (78.4)	8 (21.6)		31 (83.8)	6 (16.2)		29 (78.4)	8 (21.6)	
III–IV	25 (24.3)	78 (75.7)		37 (35.9)	66 (64.1)		34 (33)	69 (67)	
Recurrence			0.153			0.090			0.422
No	43 (42.2)	59 (57.8)		54 (52.9)	48 (47.1)		48 (47.1)	54 (52.9)	
Yes	11 (28.9)	27 (71.1)		14 (36.8)	24 (63.2)		15 (39.5)	23 (60.5)	

P. gingivalis, Porphyromonas gingivalis; CXCL2, C-X-C motif chemokine ligand 2; TANs, Tumour-associated neutrophils
$^{*}p < 0.05$; $^{**}p < 0.01$; $^{***}p < 0.001$

Signalling Technology, Inc, Boston, USA) were used in this study.

Statistical analysis

All data were expressed as mean ± SE of three independent experiments and were analysed using Student's *t*-tests or one-way analysis of variance as indicated. For analysis of clinical data, counting data were expressed by frequency and composition ratio, chi-square test was used for comparison between groups, COX regression was used to analyse the correlation between clinical indicators and death. Statistical significance was defined as $p < 0.05$ ($^{*}p < 0.05$, $^{**}p < 0.01$, and $^{***}p < 0.001$).

Results

Identification of CXCL2 as a differentially expressed gene (DEG) in the TME of OSCC infected with *P. gingivalis* by bioinformatics analyses

After merging and standardizing the two datasets, the DEGs (298 genes up and 294 genes down) were identified. (Fig. 1a, b).

The chemokine signalling pathway was identified as enriched via KEGG and GO analysis (Fig. 2a, b). The CXCL2 was a hub DEGs in the PPI network and Cytoscape (Fig. 2c, d), the neutrophil chemotaxis function was enriched by GSEA analysis (Fig. 2e).

IHC and IF staining of *P. gingivalis*, CXCL2 and TANs in the OSCC and normal oral mucosa samples

The IF double-labelling results for OSCC samples showed the location relationships of the three components, however, normal samples were negative for all three. (Fig. 3a). The IHC results for 140 OSCC samples showed that samples

Table 3 Univariate COX regression analysis of influencing factors of OSCC patients death

Variable	β	SE	Wald χ^2	HR (CI 95%)	p
Gender					
Male				1.000	
Female	−0.174	0.372	0.217	0.841 (0.405–1.744)	0.641
Age					
< 60 years				1.000	
≥ 60 years	−0.035	0.372	0.009	0.966 (0.465–2.004)	0.925
Differentiation					
Poor-moderately				1.000	
Well	−0.809	0.354	5.214	0.445 (0.222–0.892)	0.022
T stage					
T1–2				1.000	
T3–4	1.019	0.357	8.146	2.769 (1.376–5.574)	0.004
N stage					
N0				1.000	
N+	1.454	0.535	7.385	4.279 (1.5–12.209)	0.007
Clinical stage					
I–II				1.000	
III–IV	1.784	0.73	5.969	5.956 (1.423–24.929)	0.015
Recurrence					
No				1.000	
Yes	1.175	0.354	11.02	3.238 (1.618–6.48)	0.001

P. gingivalis, Porphyromonas gingivalis; CXCL2, C-X-C motif chemokine ligand 2; TANs, Tumour-associated neutrophils

*$p < 0.05$; **$p < 0.01$, ***$p < 0.001$

Table 4 Correlation analysis of the expression levels of *P. gingivalis*, CXCL2 and TANs between OSCC patients deaths

Variable		Mdel1		Model2	
		HR (95% CI)	p	HR (95% CI)	p
P. gingivalis	Weak	1.000		1.000	
	Strong	11.547 (2.758–48.346)	< 0.001	7.128 (1.562–32.537)	0.011
CXCL2	Weak	1.000		1.000	
	Strong	11.906 (3.622–39.142)	< 0.001	9.519 (2.619–34.604)	< 0.001
TANs	Weak	1.000		1.000	
	Strong	10.081 (3.067–33.138)	< 0.001	8.092 (2.253–29.063)	0.001

P. gingivalis, Porphyromonas gingivalis; CXCL2, C-X-C motif chemokine ligand 2; TANs, Tumour-associated neutrophils. No indicators were adjusted in Model 1, indicators such as T stage and recurrence were adjusted in Model 2

*$p < 0.05$; **$p < 0.01$, ***$p < 0.001$

were positive for *P. gingivalis*, CXCL2 and TANs, there were strong expression in III–IV clinical stage of OSCC, however, the weak expression in I–II clinical stage of OSCC. (Fig. 3b).

P. gingivalis, CXCL2 and TANs predicted the survival of 140 OSCC patients independently

To further evaluate the impact of *P. gingivalis*, CXCL2 and TANs in OSCC, the association between *P. gingivalis*, CXCL2 and TANs expression and patient clinicopathological parameters was investigated. In total, out of 140 primary OSCC patients, 108 were living and 32 were dead; 42 cases were poor-moderately differentiated and 98 were well differentiated; 89 cases were T1-T2 stage and 51 cases were T3-T4 stage; 50 cases were N0 stage and 90 cases were N1 stage; 37 cases were I-II stage and 103 cases were III-IV stage; 38 patients suffered from recurrence, and 102 patients were free of recurrence. Total 140 samples were divided into two groups according to the expression levels of the three indicators. *P. gingivalis*, CXCL2 and TANs high expression was found to

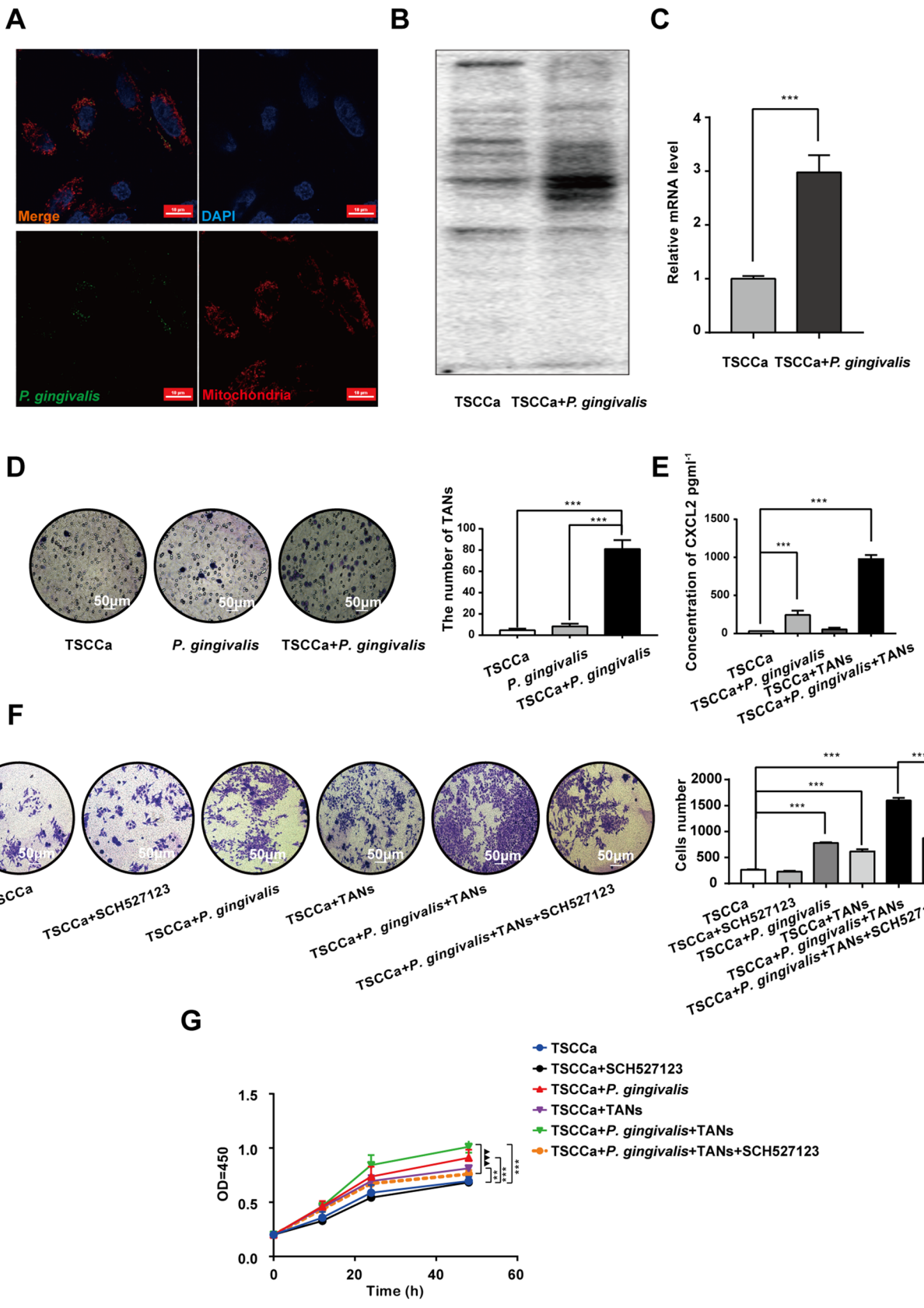
A
Merge
DAPI
P. gingivalis
Mitochondria
B
TSCCa TSCCa+P. gingivalis
C
Relative mRNA level
TSCCa TSCCa+P. gingivalis
D
50μm
TSCCa
P. gingivalis
TSCCa+P. gingivalis
The number of TANs
E
Concentration of CXCL2 pgml-1
TSCCa
TSCCa+P. gingivalis
TSCCa+TANs
TSCCa+P. gingivalis+TANs
F
TSCCa
TSCCa+SCH527123
TSCCa+P. gingivalis
TSCCa+TANs
TSCCa+P. gingivalis+TANs
TSCCa+P. gingivalis+TANs+SCH527123
Cells number
G
TSCCa
TSCCa+SCH527123
TSCCa+P. gingivalis
TSCCa+TANs
TSCCa+P. gingivalis+TANs
TSCCa+P. gingivalis+TANs+SCH527123
OD=450
Time (h)

◂**Fig. 4** The verification of cell coculture models and experiments assessing cell biological behaviour. **a** *P. gingivalis* was marked by the fluorochrome of SYTO9, the nucleus was marked by DAPI, and the mitochondria were marked by MitoTracker red. **b** The difference in the expression of *P. gingivalis* protein between the coculture cell model and the TSCCa cell model was detected by Western blotting. **c** The difference in the expression of *P. gingivalis* mRNA between the coculture cell model and the TSCCa cell model was detected by qRT-PCR. **d** A neutrophil chemotaxis experiment was used to detect the chemotactic ability of TANs in the supernatants of TSCCa, *P. gingivalis*, and TSCCa + *P. gingivalis* culture systems. **e** The content of CXCL2 in the supernatants of TSCCa, TSCCa + *P. gingivalis*, TSCCa + TANs and TSCCa + *P. gingivalis* + TANs coculture systems. **f**, **g** Invasion and CCK-8 assays were used to detect the differences in cell invasion and proliferation in the TSCCa, TSCCa + SCH527123, TSCCa + *P. gingivalis*, TSCCa + TANs, TSCCa + *P. gingivalis* + TANs and TSCCa + *P. gingivalis* + TANs + SCH527123 groups (**$p < 0.01$, ***$p < 0.001$ and ▲▲▲$p < 0.001$; one-way analysis of variance, Student's *t*-test)

be correlated with clinical indicators. (Table 2). Furthermore, multivariate Cox-regression analysis illustrated that *P. gingivalis*, CXCL2 and TANs were an independent prognostic factor for OSCC. (Tables 3, 4 and Fig. 3c).

Development of a coculture cell model of *P. gingivalis* and TSCCa cells and biological behaviour assays of cell models

The coculture model was established successfully (Fig. 4a). The protein level of *P. gingivalis* in the coculture group was significantly higher than that in the TSCCa cells group (Fig. 4b). The mRNA level of *P. gingivalis* in the coculture group was also significantly higher than that in the TSCCa cells group ($p < 0.001$) (Fig. 4c).

TANs were treated with the supernatant of TSCCa, *P. gingivalis* and TSCCa + *P. gingivalis* cultures, and the results showed that the supernatant of the TSCCa + *P. gingivalis* culture had the strongest chemotactic ability to TANs (Fig. 4d). The CXCL2 protein levels of the supernatant of the TSCCa + *P. gingivalis* + TANs culture were significantly higher than those of the TSCCa ($p < 0.001$) and TSCCa + *P. gingivalis* cultures ($p < 0.001$) (Fig. 4e). The invasion and proliferation capacities of TSCCa cells improved significantly in the TSCCa + *P. gingivalis* + TANs group. After using SCH527123, the invasion and proliferation capacities of TSCCa cells were reduced significantly (Fig. 4f, g).

P. gingivalis promotes OSCC tumour progression via CXCL2/CXCR2 axis in C57BL/6 mouse models

A diagram of our experimental protocol is shown (Fig. 5a). The tumours of the experimental group were significantly larger than those of the control group. When SCH527123 was used for treatment, the tumour volume of the treatment group was reduced compared with that of the experimental group. Compared with that in the low-dose treatment group, the tumour inhibition in the high-dose treatment group was more obvious (Fig. 5b). Successful generation of the tumour-bearing mouse model was confirmed by HE staining. IHC showed that the expression of *P. gingivalis* was negative in the control group but positive in the experimental group (Fig. 5c). The IF double-labelling of mouse model samples showed that the levels of CXCL2 and TANs in the experimental group were higher than those in the control group; in the low-dose treatment group, the levels of CXCL2 and TANs were lower than those in the experimental group. In the high-dose treatment group, the levels of CXCL2 and TANs were significantly lower than those in the experimental group. In addition, in the high-dose treatment group, the levels of CXCL2 and TANs were lower than those in the low-dose treatment group (Fig. 5d).

The CXCL2/CXCR2 axis is activated by *P. gingivalis* and induces the EMT phenotype via the JAK1/STAT3 signalling pathway

The protein levels of CXCL2, CXCR2, JAK1, STAT3, p-JAK1, p-STAT3, and N-cadherin were significantly increased, however, the protein levels of E-cadherin were significantly decreased as shown by Western blot analysis, which means that the EMT phenotype was presented and the signalling pathway of JAK1/STAT3 was activated in the group of TSCCa + *P. gingivalis* + TANs (Fig. 6a).

CXCL2/CXCR2 knockdown inhibits the activation level of the JAK1/STAT3 signalling pathway and reverses the EMT phenotype of OSCC cells

CXCL2 and CXCR2 lentiviruses were transfected into a cocultured cell model (Fig. 6b). The knockdown level was verified by qRT—PCR and Western blotting (Fig. 6c, d). The lentiviruses of sh-CXCL2 and sh-CXCR2 were co-transfected into TSCCa cells (Fig. 7a). Flow cytometry was used to screen out the positive cells that expression both lentiviruses of sh-CXCL2 and sh-CXCR2 (Fig. 7b). The cloned of positive cells were screen out by limited dilution method (Fig. 7c). Four different cell models were established using sh-CXCL2/CXCR2 lentivirus-positive cells. At the molecular level, the activation of JAK1/STAT3 was decreased, and the phenotype of EMT was reversed according to Western blot assays (Fig. 7d).

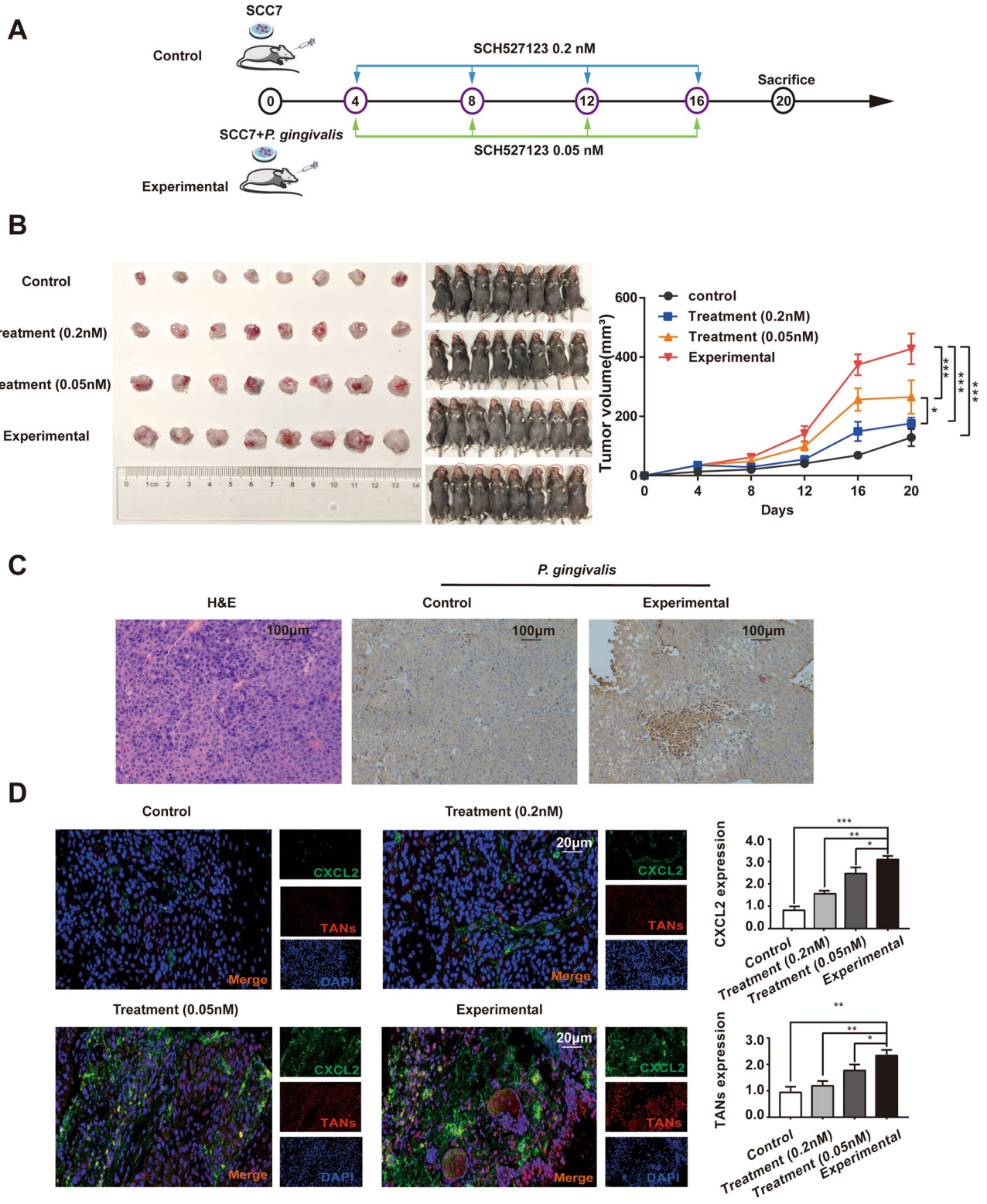
A
SCC7
Control
SCH527123 0.2 nM
Sacrifice
0
4
8
12
16
20
SCC7+P. gingivalis
SCH527123 0.05 nM
Experimental
B
Control
Treatment (0.2nM)
Treatment (0.05nM)
Experimental
control
Treatment (0.2nM)
Treatment (0.05nM)
Experimental
Tumor volume(mm³)
600
400
200
0
0
4
8
12
16
20
Days
*
***
**
**
***
C
P. gingivalis
H&E
Control
Experimental
100μm
100μm
100μm
D
Control
Treatment (0.2nM)
Treatment (0.05nM)
Experimental
CXCL2
TANs
DAPI
Merge
20μm
CXCL2 expression
TANs expression
4.0
3.0
2.0
1.0
0.0
Control
Treatment (0.2nM)
Treatment (0.05nM)
Experimental
***
**
*

◂**Fig. 5** Tumour bearing experiment in C57BL/6 mice. **a** Experimental scheme in which C57BL/6 mice were used to establish animal models. The experiment was divided into four groups: the control group (SCC7), experimental group (SCC7 + *P. gingivalis*), low-dose treatment group (SCC7 + *P. gingivalis* + 0.05 nM SCH527123), and high-dose treatment group (SCC7 + *P. gingivalis* + 0.20 nM SCH527123). The treatment group was injected with different doses of SCH527123 at the site of tumour cell inoculation at 4, 8, 12 and 16 days. Mice were sacrificed at 20 days. **b** In the control group, the tumour volume of mice killed on day 20 was less than that of mice in other three groups; in the experimental group, the tumour volume increased significantly compared with the control group, and continued to increase with the extension of time; when SCH527123 was used for treatment, it was found that the tumour volume in the low-dose treatment group was less than that in the experimental group. Similarly, compared with that in the experimental group, the tumour volume in the high-dose treatment group also decreased. Comparing the high-dose treatment group with the low-dose treatment group, it was found that the tumour inhibition was more obvious in the former. **c**. The tumour-bearing mouse model samples were assessed by HE staining and IHC. The IHC results showed that the expression of *P. gingivalis* was negative in the control group (SCC7) and positive in the experimental group (SCC7 + *P. gingivalis*). **d**. IF showed that CXCL2 and TANs were both expressed in the control group, and the levels of CXCL2 and TANs in the experimental group were higher than those in the control group. The levels of CXCL2 and TANs in the low-dose treatment group were lower than those in the experimental group. In the high-dose treatment group, the levels of CXCL2 and TANs were significantly lower than those in the low-dose treatment group. (*$p < 0.05$, **$p < 0.01$, and ***$p < 0.001$; one-way analysis of variance).

Discussion

The oral microbiota plays an important role in promoting the development of OSCC through mediating the direct metabolism of chemical carcinogens and the systemic inflammatory response [23]. Oral microbiota such as *P. gingivalis* can destroy the local immune response by establishing chronic inflammation and can lead to the immune escape of tumour cells [24]. In this study, we have evidenced that when *P. gingivalis* infects the TME of OSCC, the novel CXCL2/CXCR2/JAK1/STAT3 signalling pathway is crucial for the progression and EMT phenotype acquisition of OSCC cells. Our initial study has screened out the CXCL2 was not only a hub DEGs but also a hub gene in the PPI network from the two datasets has been merged. Moreover, the neutrophil chemotaxis related signalling pathway and gene function were enriched by GO, KEGG and GSEA analysis. Previous studies have reported that *P. gingivalis* induced the production of reactive oxygen species, CXCL8 and CCL2 by neutrophils to deteriorate periodontitis [25]. Key periodontal pathogens *P. gingivalis* and *F. nucleatum* could enhance OSCC cell migration, invasion, stemness and tumour aggressivity [26]. Based on the results of our bioinformatics analysis and previous studies, we speculated that elevated *P. gingivalis* infected OSCC samples may exacerbate the OSCC progression via CXCL2/CXCR2 axis to recruit TANs. To verify this assumption, we then evaluated the expression of *P. gingivalis* in OSCC samples. We found that the *P. gingivalis*, CXCL2 and TANs were positive expression in OSCC samples and negative expression in normal samples. Moreover, the strong expression of *P. gingivalis*, CXCL2 and TANs in OSCC patients may be tightly relate to the poor prognosis of OSCC patients.

It is well known that *P. gingivalis* has been reported to disrupt the normal immune response of the host and is associated with the progression of OSCC by regulating the immune response [27]. Recently, it has been reported that CXCL2 can promote the occurrence of colorectal cancer by recruiting myeloid-derived suppressor cells (MDSCs) to increase their abundance [28]. Studies have pointed out that neutrophils in the TME increased the invasiveness of OSCC, because the oral cavity has a constant population of neutrophils, in specific inflammatory states, including periodontal disease [29, 30]. Although a large number of studies have confirmed the close relationship between *P. gingivalis* and OSCC, few studies have analysed the molecular mechanism by which *P. gingivalis* promotes tumour progression in the TME of OSCC. As the TANs recruited from TME when *P. gingivalis* infected, the TME may have the potential for pro-tumour effect. Because of a numerous inflammatory cytokines were released, various types of immune cells were recruited increasingly and to form a positive loop to further promote tumour progression. For determining the chemotactic ability of *P. gingivalis* to TANs, the coculture cell models were constructed and then we found that the protein and mRNA expression level of CXCL2 and the chemotaxis ability were evaluated seriously compare to control groups. In our study, *P. gingivalis* was found to invade and colonize tumour cells and by building the cells and animal model, the ability of *P. gingivalis* on promoting tumour progression were assessed in vitro and in vivo, we found that the *P. gingivalis* could promote the invasion and proliferation of tumour cells, and promote tumour progression in tumour-bearing mice. Human papillomavirus (HPV) is a key pathogenic factor that facilitates OSCC formation by establishing a coculture system between microbiota and tumour cells [31]. This is consistent with the conclusion that *P. gingivalis* can promote the aggressive phenotype of tumour cells in the present study.

Chemotactic factors have been identified as kinds of key regulator of tumour progression, by binding to corresponding receptors, they activate various kinds of immune cells [32]. CXCL2 is a secreted chemokine that mainly produced by tumour cells, neutrophils, macrophages, and pathogenic microorganisms [33], CXCL2 interacts with its receptor CXCR2 to regulator biological functions, CXCL2/CXCR2 axis could activates a board spectrum downstream signalling, such as JAK1/STAT3, PI3K/AKT and MAPK/p38 etc. [34]. Although the effect of CXCL2/CXCR2 and its

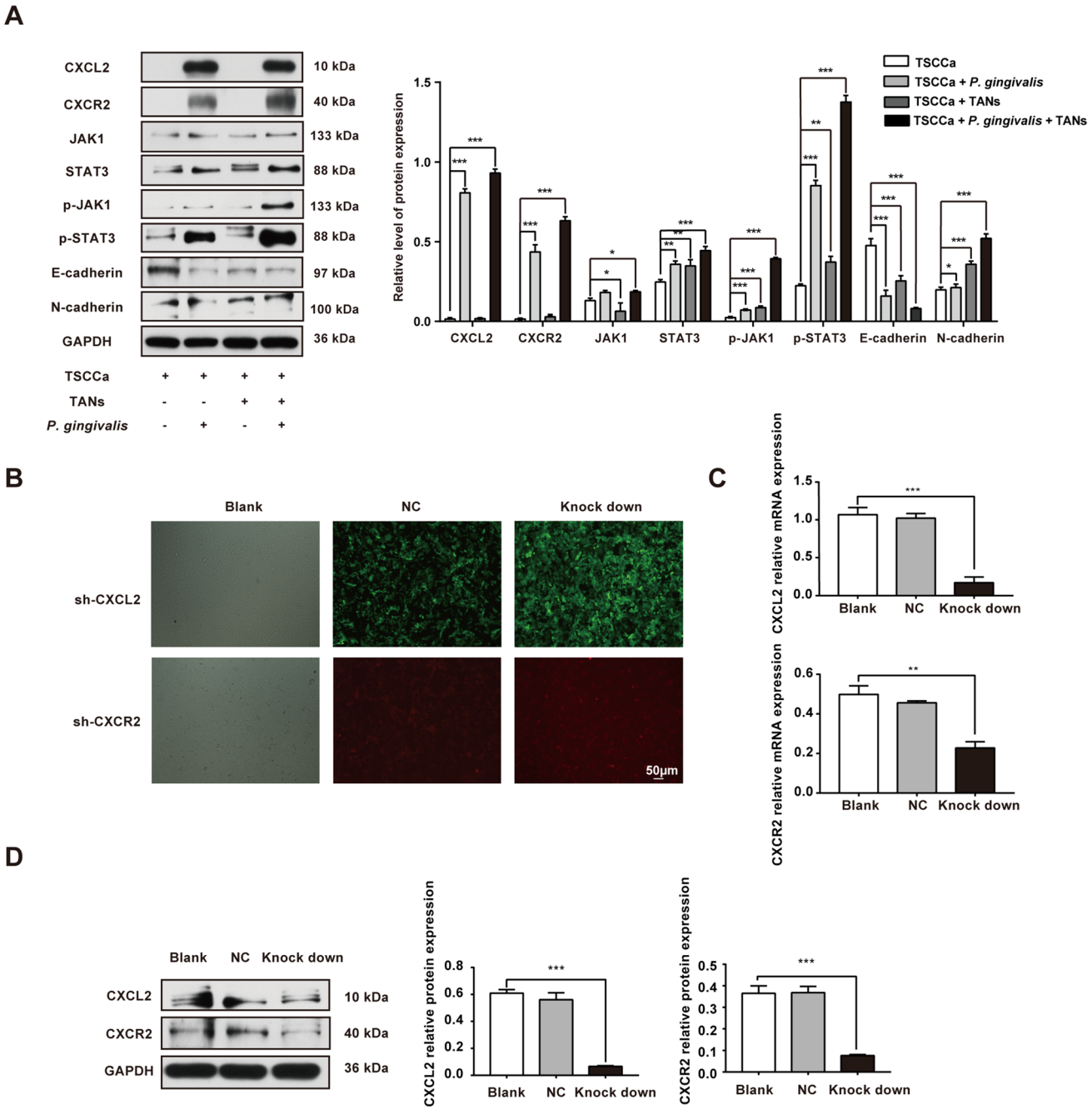

Fig. 6 Acquisition of the EMT phenotype was verified by activation of the JAK1/STAT3 signalling pathway through the CXCL2/CXCR2 signalling axis. **a** Western blot analysis showed that EMT occurred and the JAK1/STAT3 signalling pathway was activated by CXCL2/CXCR2 when *P. gingivalis* infected the TME of OSCC. **b** After coculture for 24 h, and the cells were transinfected with sh-CXCL2 and sh-CXCR2 lentiviruses for 72 h, the cells were observed under a fluorescence microscope. **c**, **d** Knockdown of CXCL2 and CXCR2 was verified at the protein and mRNA levels by Western blotting and qRT-PCR

downstream signalling pathways on tumour progression has been studied for years, the biofunction of CXCL2 in OSCC is still unclear. In our study, we found that CXCL2/CXCR2 axis and its downstream signalling, both JAK1/STAT3 and EMT phenotype were activated after the TME was infected by *P. gingivalis*. In addition, the biological behaviour of tumour cells and the tumour volume of tumour-bearing mice were reduced clearly by specific CXCL2/CXCR2 inhibitor application. Moreover, immunofluorescence showed that the expression of CXCL2 and TANs were significantly reduced in tumour-bearing samples of mice.

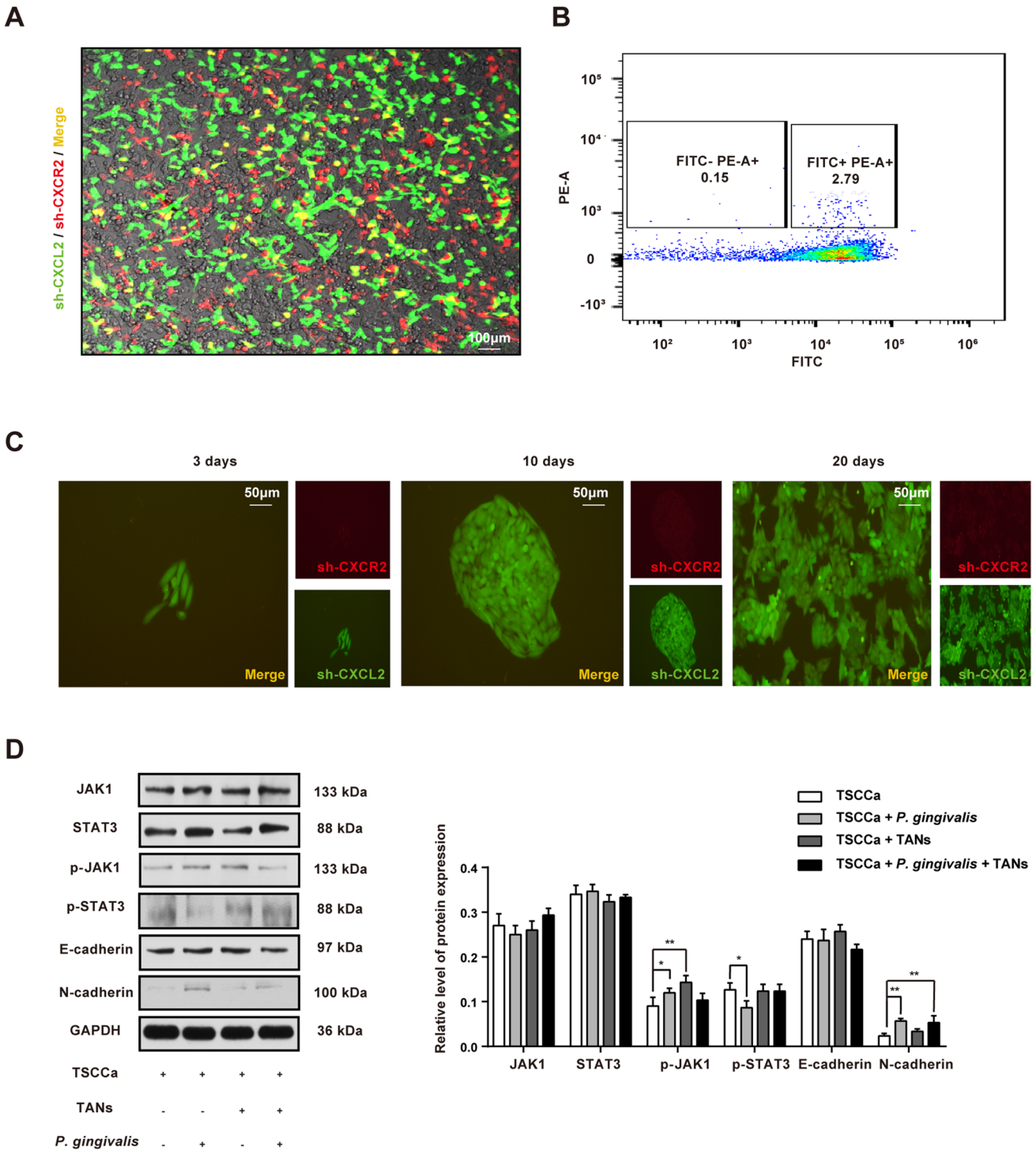

Fig. 7 Screening and culture of positive clone cells expressing both the lentiviruses of sh-CXCL2 and sh-CXCR2 which can reverse the phenotype of EMT and rescue the signalling pathway of JAK1/STAT3. **a** The lentiviruses of sh-CXCL2 and sh-CXCR2 were co-transfected into TSCCa cells. **b** Flow cytometry was used to screen out the positive cells that expression both lentiviruses of sh-CXCL2 and sh-CXCR2. **c** The clone of positive cells were screened out and cultured by limited dilution method. **d** Western blot analysis after inactivation of the CXCL2/CXCR2 signalling axis in the *P. gingivalis*-infected TME of OSCC, the activity of the JAK1/STAT3 signalling pathway was decreased, and the EMT process was reversed. (*$p < 0.05$, **$p < 0.01$, and ***$p < 0.001$; one-way analysis of variance)

The CXCL2/CXCR1 signalling axis has been found to promote tumour progression by mediating angiogenesis in different types of tumours [35]. CXCR2, as a nonspecific receptor for CXCL2, has been proven to promote tumour development in a variety of tumours [36]. We targeted the CXCL2/CXCR2 signalling axis and blocked the expression of this signalling axis through lentivirus interference, resulting in the reversal of the highly invasive phenotype of cells and reduced activation of the JAK1/STAT3 signalling pathway. Small molecule inhibitors are promising targeted therapies, and after oral administration of SCH527123 inhibitor to transplanted tumour-bearing mice, the tumour volume was decreased significantly, suggesting that SCH527123 may be a promising drug for melanoma treatment [37]. Our study verified that inhibition of the signalling axis can indeed reduce the proliferation and invasion of OSCC cells at the cellular and animal levels and demonstrated the molecular mechanisms involved.

In summary, *P. gingivalis* promotes OSCC progression by recruiting TANs by increasing the secretion of CXCL2 in the TME of OSCC. These findings suggest that *P. gingivalis* may be a potential risk factor for poor prognosis in OSCC patients. The CXCL2/CXCR2 signalling axis may be a new potential target for the management of OSCC patients with severe periodontal disease.

Supplementary Information The online version contains supplementary material available at https://doi.org/10.1007/s00262-022-03348-5.

Acknowledgements Not applicable.

Authors' contributions ZCGo conceived and designed the study. ZCGu conducted the experiments. SJ and SLJ performed the statistical analysis. ZCGu wrote the manuscript. ZCGu reviewed and edited the manuscript. All authors agree to be accountable for all aspects of the research in ensuring that the accuracy or integrity of any part of the work are appropriately investigated and resolved. All authors read and approved the final manuscript.

Funding This study was supported by 1. National Natural Science Foundation of China, (Project Number: 82160189); 2. The project of Tianshan Innovation Team of Xinjiang Uygur Autonomous Region, (Project Number: 202110755).

Availability of data and materials The data used to support the findings of this study are available from the corresponding author upon request.

Declarations

Conflict of interests The authors declare no potential conflict of interests.

Ethics approval and consent to participate Written informed consent was obtained from all OSCC patients. All clinical experiments were approved by the institutional ethical review board of XinJiang Medical University (Approval No. IACUC20180411-13). All animal researches adhere to the ARRIVE guidelines (https://arriveguidelines.org/arrive-guidelines), and were approved by the Ethics Committee of The First Affiliated Hospital of XinJiang Medical University.

Consent for publication Not applicable.

Manuscript statement A preprint has previously been published [40].

References

1. Johnson DE, Burtness B, Leemans CR, Lui VWY, Bauman JE, Grandis JR (2020) Head and neck squamous cell carcinoma. Nat Rev Dis Primers 6:92–113. https://doi.org/10.1038/s41572-020-00224-3
2. Siegel RL, Miller KD, Fuchs HE, Jemal A (2021) Cancer statistics, 2021. CA: Cancer J Clin 71:7–33. https://doi.org/10.3322/caac.21654
3. Liu J, Jiang X, Zou A, Mai Z, Huang Z, Sun L, Zhao J (2021) circIGHG-induced epithelial-to-mesenchymal transition promotes oral squamous cell carcinoma progression via miR-142-5p/IGF2BP3 signaling. Can Res 81:344–355. https://doi.org/10.1158/0008-5472.Can-20-0554
4. Amieva M, Peek RM Jr (2016) Pathobiology of helicobacter pylori-induced gastric cancer. Gastroenterology 150:64–78. https://doi.org/10.1053/j.gastro.2015.09.004
5. Inaba H, Sugita H, Kuboniwa M, Iwai S, Hamada M, Noda T, Morisaki I, Lamont RJ, Amano A (2014) Porphyromonas gingivalis promotes invasion of oral squamous cell carcinoma through induction of proMMP9 and its activation. Cell Microbiol 16:131–145. https://doi.org/10.1111/cmi.12211
6. Liu XB, Gao ZY, Sun CT, Wen H, Gao B, Li SB, Tong Q (2019) The potential role of *P. gingivalis* in gastrointestinal cancer: a mini review. Infect Agents Cancer 14:23. https://doi.org/10.1186/s13027-019-0239-4
7. Irfan M, Delgado RZR, Frias-Lopez J (2020) The oral microbiome and cancer. Front Immunol 11:591088. https://doi.org/10.3389/fimmu.2020.591088
8. Libby P (2007) Inflammatory mechanisms: the molecular basis of inflammation and disease. Nutr Rev 65:S140–S146. https://doi.org/10.1111/j.1753-4887.2007.tb00352.x
9. Kraus RF, Gruber MA (2021) Neutrophils-from bone marrow to first-line defense of the innate immune system. Front Immunol 12:767175. https://doi.org/10.3389/fimmu.2021.767175
10. Giese MA, Hind LE, Huttenlocher A (2019) Neutrophil plasticity in the tumor microenvironment. Blood 133:2159–2167. https://doi.org/10.1182/blood-2018-11-844548
11. Sahingur SE, Yeudall WA (2015) Chemokine function in periodontal disease and oral cavity cancer. Front Immunol 6:214. https://doi.org/10.3389/fimmu.2015.00214
12. Vashishta A, Jimenez-Flores E, Klaes CK, Tian S, Miralda I, Lamont RJ, Uriarte SM (2019) Putative Periodontal Pathogens, Filifactor Alocis and Peptoanaerobacter Stomatis, induce differential cytokine and chemokine production by human neutrophils. Pathogens (Basel, Switzerland). https://doi.org/10.3390/pathogens8020059
13. Chen Y, Shao Z, Jiang E et al (2020) CCL21/CCR7 interaction promotes EMT and enhances the stemness of OSCC via a JAK2/STAT3 signaling pathway. J Cell Physiol 235:5995–6009. https://doi.org/10.1002/jcp.29525
14. Hardaway AL, Herroon MK, Rajagurubandara E, Podgorski I (2015) Marrow adipocyte-derived CXCL1 and CXCL2 contribute

to osteolysis in metastatic prostate cancer. Clin Exp Metas 32:353–368. https://doi.org/10.1007/s10585-015-9714-5
15. Acharyya S, Oskarsson T, Vanharanta S et al (2012) A CXCL1 paracrine network links cancer chemoresistance and metastasis. Cell 150:165–178. https://doi.org/10.1016/j.cell.2012.04.042
16. Yu H, Lee H, Herrmann A, Buettner R, Jove R (2014) Revisiting STAT3 signalling in cancer: new and unexpected biological functions. Nat Rev Cancer 14:736–746. https://doi.org/10.1038/nrc3818
17. Wang J, Lv X, Guo X et al (2021) Feedback activation of STAT3 limits the response to PI3K/AKT/mTOR inhibitors in PTEN-deficient cancer cells. Oncogenesis 10:8. https://doi.org/10.1038/s41389-020-00292-w
18. Geng F, Liu J, Guo Y, Li C, Wang H, Wang H, Zhao H, Pan Y (2017) Persistent exposure to *Porphyromonas gingivalis* promotes proliferative and invasion capabilities, and tumorigenic properties of human immortalized oral epithelial cells. Front Cell Infect Microbiol 7:57. https://doi.org/10.3389/fcimb.2017.00057
19. Qiu X, Lei Z, Wang Z, Xu Y, Liu C, Li P, Wu H, Gong Z (2019) Knockdown of LncRNA RHPN1-AS1 inhibits cell migration, invasion and proliferation in head and neck squamous cell carcinoma. J Cancer 10:4000–4008. https://doi.org/10.7150/jca.29029
20. Guo ZC, Jumatai S, Jing SL, Hu LL, Jia XY, Gong ZC (2021) Bioinformatics and immunohistochemistry analyses of expression levels and clinical significance of CXCL2 and TANs in an oral squamous cell carcinoma tumor microenvironment of *Porphyromonas gingivalis* infection. Oncol Lett 21:189. https://doi.org/10.3892/ol.2021.12450
21. Schmid MC, Khan SQ, Kaneda MM et al (2018) Integrin CD11b activation drives anti-tumor innate immunity. Nat Commun 9:5379. https://doi.org/10.1038/s41467-018-07387-4
22. Xue Y, Du HD, Tang D et al (2019) Correlation between the NLRP3 inflammasome and the prognosis of patients with LSCC. Front Oncol 9:588. https://doi.org/10.3389/fonc.2019.00588
23. Vyhnalova T, Danek Z, Gachova D, Linhartova PB (2021) The role of the oral microbiota in the etiopathogenesis of oral squamous cell carcinoma. Microorganisms. https://doi.org/10.3390/microorganisms9081549
24. Whitmore SE, Lamont RJ (2014) Oral bacteria and cancer. PLoS Pathog 10:e1003933. https://doi.org/10.1371/journal.ppat.1003933
25. Damgaard C, Kantarci A, Holmstrup P, Hasturk H, Nielsen CH, Van Dyke TE (2017) Porphyromonas gingivalis-induced production of reactive oxygen species, tumor necrosis factor-α, interleukin-6, CXCL8 and CCL2 by neutrophils from localized aggressive periodontitis and healthy donors: modulating actions of red blood cells and resolvin E1. J Periodontal Res 52:246–254. https://doi.org/10.1111/jre.12388
26. Kamarajan P, Ateia I, Shin JM, Fenno JC, Le C, Zhan L, Chang A, Darveau R, Kapila YL (2020) Periodontal pathogens promote cancer aggressivity via TLR/MyD88 triggered activation of Integrin/FAK signaling that is therapeutically reversible by a probiotic bacteriocin. PLoS Pathog 16:e1008881. https://doi.org/10.1371/journal.ppat.1008881
27. Ibáñez L, de Mendoza I, MaritxalarMendia X, García de la Fuente AM, Quindós Andrés G, Aguirre Urizar JM (2020) Role of Porphyromonas gingivalis in oral squamous cell carcinoma development: a systematic review. J Periodontal Res 55:13–22. https://doi.org/10.1111/jre.12691
28. Harusato A, Viennois E, Etienne-Mesmin L et al (2019) Early-life microbiota exposure restricts myeloid-derived suppressor cell-driven colonic tumorigenesis. Cancer Immunol Res 7:544–551. https://doi.org/10.1158/2326-6066.Cir-18-0444
29. Glogauer JE, Sun CX, Bradley G, Magalhaes MA (2015) Neutrophils increase oral squamous cell carcinoma invasion through an invadopodia-dependent pathway. Cancer Immunol Res 3:1218–1226. https://doi.org/10.1158/2326-6066.Cir-15-0017
30. Lakschevitz FS, Aboodi GM, Glogauer M (2013) Oral neutrophils display a site-specific phenotype characterized by expression of T-cell receptors. J Periodontol 84:1493–1503. https://doi.org/10.1902/jop.2012.120477
31. El-Bayoumy K, Christensen ND, Hu J et al (2020) An Integrated approach for preventing oral cavity and oropharyngeal cancers: two etiologies with distinct and shared mechanisms of carcinogenesis. Cancer Prev Res (Philadelphia, PA) 13:649–660. https://doi.org/10.1158/1940-6207.Capr-20-0096
32. Zhang Q, Wang J, Yao X et al (2021) Programmed cell death 10 mediated CXCL2-CXCR2 signaling in regulating tumor-associated microglia/macrophages recruitment in glioblastoma. Front Immunol 12:637053. https://doi.org/10.3389/fimmu.2021.637053
33. Lin T, Zhang E, Mai PP, Zhang YZ, Chen X, Peng LS (2021) CXCL2/10/12/14 are prognostic biomarkers and correlated with immune infiltration in hepatocellular carcinoma. Biosci Rep. https://doi.org/10.1042/bsr20204312
34. Grépin R, Guyot M, Giuliano S et al (2014) The CXCL7/CXCR1/2 axis is a key driver in the growth of clear cell renal cell carcinoma. Can Res 74:873–883. https://doi.org/10.1158/0008-5472.Can-13-1267
35. Wei ZW, Xia GK, Wu Y et al (2015) CXCL1 promotes tumor growth through VEGF pathway activation and is associated with inferior survival in gastric cancer. Cancer Lett 359:335–343. https://doi.org/10.1016/j.canlet.2015.01.033
36. Susek KH, Karvouni M, Alici E, Lundqvist A (2018) The Role of CXC Chemokine Receptors 1–4 on immune cells in the tumor microenvironment. Front Immunol 9:2159. https://doi.org/10.3389/fimmu.2018.02159
37. Chapman RW, Minnicozzi M, Celly CS et al (2007) A novel, orally active CXCR1/2 receptor antagonist, Sch527123, inhibits neutrophil recruitment, mucus production, and goblet cell hyperplasia in animal models of pulmonary inflammation. J Pharmacol Exp Ther 322:486–493. https://doi.org/10.1124/jpet.106.119040
38. Lee J, Roberts JS, Atanasova KR, Chowdhury N, Han K, Yilmaz Ö (2017) Human primary epithelial cells acquire an epithelial-mesenchymal-transition phenotype during long-term infection by the oral opportunistic pathogen, *Porphyromonas gingivalis*. Front Cell Infect Microbiol 7:493. https://doi.org/10.3389/fcimb.2017.00493
39. Holz O, Khalilieh S, Ludwig-Sengpiel A, Watz H, Stryszak P, Soni P, Tsai M, Sadeh J, Magnussen H (2010) SCH527123, a novel CXCR2 antagonist, inhibits ozone-induced neutrophilia in healthy subjects. Eur Respir J 35:564–570. https://doi.org/10.1183/09031936.00048509
40. Guo Z, Jing S-l, Jumatai S et al (2022) Porphyromonas gingivalis promotes the progression of oral squamous cell carcinoma by activating the neutrophil chemotaxis in the tumor microenvironment, PREPRINT (Version 1) available at Research Square https://doi.org/10.21203/rs.3.rs-1663147/v1